DAMAGE DIAGNOSIS USING EXPERIMENTAL RITZ VECTORS

By Hoon Sohn[1] and Kincho H. Law[2]

ABSTRACT: This paper describes an experimental study on the use of Ritz vectors for damage detection of a grid-type bridge model. A new procedure to extract Ritz vectors from experimental modal analysis is proposed and demonstrated using the test structure. The extracted Ritz vectors are then used for the damage detection of the test structure using a Bayesian probabilistic approach. Using appropriate load patterns, Ritz vectors can be made more sensitive to damage than modal vectors. The results indicate that the use of load-dependent Ritz vectors produce better damage diagnoses than the modal vectors. The Bayesian probabilistic approach is shown to give better diagnostic results than commonly used deterministic methods.

INTRODUCTION

Damage detection and health monitoring of large-scale structures are important challenges to engineering research. One common approach is to employ vibration characteristics of a structure to predict the damage locations and to estimate the amount of damage (Doebling et al. 1996). It has, however, been shown that damage in an early stage may not cause significant changes in the modal parameters.

To overcome the sensitivity problems of modal vectors to damage, several alternatives have been proposed. Pandey et al. (1991) proposed to compute the mode shape curvature from the displacement mode shape and demonstrated that the changes in the mode shape curvature can be a good indicator of damage for beam structures. Topole and Stubbs (1995) presented a damage index method to measure the decrease of modal strain energy before and after damage occurrence. Yao et al. (1992) employed the strain mode shape, which is related to the force redistribution, to identify local damage of a braced steel frame structure. These aforementioned methods require the direct measurement of dynamic strain or the derivative of the measured displacement mode shape to compute the strain mode shape or mode shape curvature. However, the noise induced by the measurement of dynamic strains is generally higher than that from typical accelerometer measurement. Numerical procedures to compute the curvature from displacement also inevitably produce errors.

This paper describes the use of Ritz vectors obtained from imposing different load patterns for damage detection. Ritz vectors have been shown to have many potential advantages in structural dynamics over modal parameters. For linear dynamic analysis, the response quantities of interest can be approximated more effectively by a smaller number of Ritz vectors than the modal vectors (Nour-Omid and Clough 1984; Leger et al. 1986). In numerical analysis, Ritz (or Lanczos) vectors have been used to find partial extremal solutions of large eigenvalue problems (Golub and Loan 1996) and to reanalyze a structural system with localized modifications (Carey et al. 1994). Recent studies have shown that it is possible to experimentally extract Ritz vectors from the traditional modal analysis (Cao and Zimmerman 1997b). However, very few studies have applied Ritz vectors to damage detection problems (Cao and Zimmerman 1997a; Sohn and Law 2000).

In this paper, Ritz vectors are incorporated into a Bayesian probabilistic framework for a damage detection problem (Sohn and Law 1997). The applicability of this approach is investigated using a grid-type bridge model constructed and tested at the Hyundai Institute of Construction Technology, Kyunggi-Do, South Korea. A new extraction procedure of Ritz vectors based on a measured flexibility matrix is also presented. The estimated Ritz vectors are then applied to perform the damage diagnosis for the test structure. Finally, the diagnostic results obtained from the Bayesian approach are compared with those by other damage detection methods.

EXPERIMENTAL BRIDGE MODEL

The steel bridge model employed in this experimental study consists of two parallel girders and six evenly spaced cross beams connecting the two girders, as shown in Fig. 1. The girders are steel rectangular tubes and the cross beams are C-shaped members. Using impact excitations, one extracts Ritz and modal vectors from the vibration response of the test structure.

An SA-390 signal analyzer with four channels is used for the analog-to-digital conversion of accelerometer signals and the fast Fourier transform calculation. Data acquisition parameters are specified such that a frequency response function (FRF) in the range of 0–100 Hz could be estimated. Each spectrum is computed by averaging three 8-s time histories; 2,048 points are sampled for 8 s and this sampling rate produces a frequency resolution of 0.125 Hz. An exponential window is applied to all measured time histories prior to the fast Fourier transform calculation.

A Dytran 5801A4 impact hammer and three Dytran 3100B accelerometers with a normal sensitivity of 100 mV/g are used. The excitation is applied at nodes 3–5, one at a time, as shown in Fig. 2. The sensors measure the vertical accelerations at the 12 nodes as indicated in Fig. 2.

Note that, because the SA-390 data acquisition system has only four channels and there are three accelerometers, the first channel is always connected to the input hammer and the remaining three channels are connected to the three accelerometers. To complete one set of the modal test, the hammer excitation is repeated 12 times at one point and the three accelerometers are moved from one set of three nodes to another set of three nodes after every three excitations. (Note that each FRF is computed by averaging the three response time histories and there are 12 measurement points and three accelerometers.) The rational polynomial (Richardson and Formenti 1982) technique is employed to extract the first six natural frequencies and the corresponding modal vectors from the recorded FRFs.

EXTRACTION OF RITZ VECTORS

In this section, a procedure to extract Ritz vectors from a flexibility matrix constructed using measured vibration data is

[1]Tech. Staff Member, Engrg. Sci. and Applications Div., Engrg. Anal. Group, Los Alamos Nat. Lab., Los Alamos, NM 87545. E-mail: sohn@lanl.gov

[2]Prof., Dept. of Civ. and Envir. Engrg., Stanford Univ., Stanford, CA 94305-4020.

Note. Associate Editor: Ahsan Kareem. Discussion open until April 1, 2002. To extend the closing date one month, a written request must be filed with the ASCE Manager of Journals. The manuscript for this paper was submitted for review and possible publication on August 3, 1999; revised August 2, 2001. This paper is part of the ***Journal of Engineering Mechanics***, Vol. 127, No. 11, November, 2001. ©ASCE, ISSN 0733-9399/01/0011-1184–1193/$8.00 + $.50 per page. Paper No. 21575.

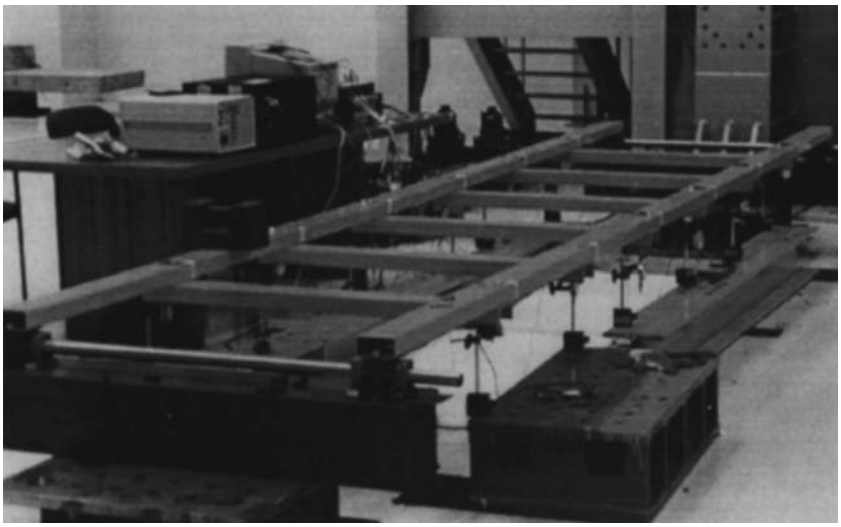

FIG. 1. Grid-Type Bridge Model

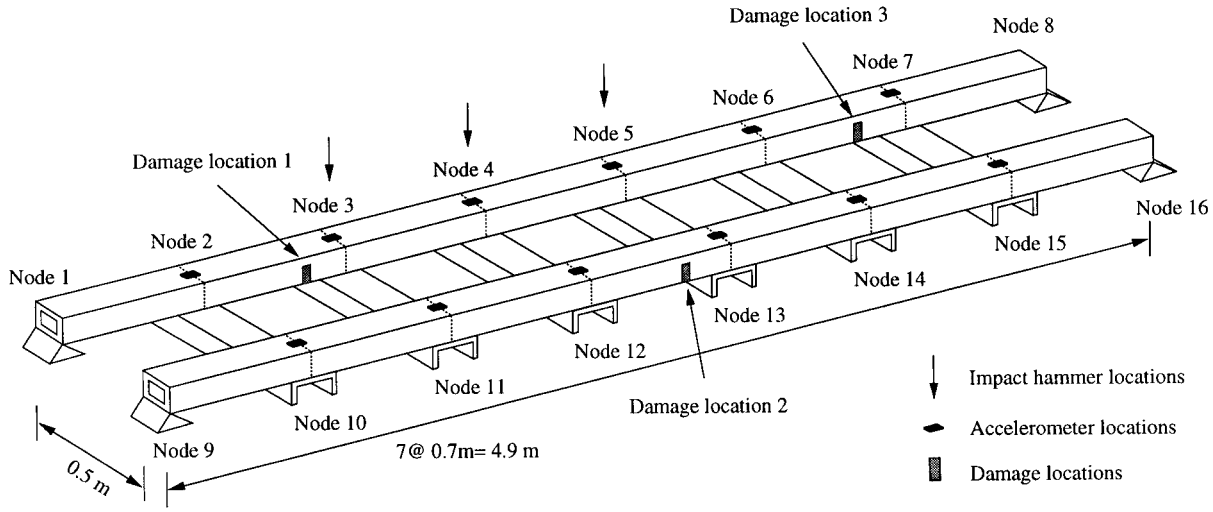

FIG. 2. Impact, Accelerometer, and Damage Locations of Grid-Type Bridge Structure

presented. Following the numerical procedures typically used in generating the Ritz or Lanczos vectors [for example, Leger et al. (1986) and Cao and Zimmerman (1997b)], the Ritz vectors are computed using the inverse of the stiffness matrix, hereby called the flexibility matrix **F**, rather than the stiffness matrix itself. It has been shown that a flexibility matrix can be constructed using vibration test data (Raghavendrachar and Aktan 1992; Doebling 1995). Thus, it is a natural extension to extract Ritz vectors based on a measured flexibility matrix.

The extraction of Ritz vectors starts with the assumption that the dynamic loading $\mathbf{F}(t)$ can be separated into a spatial load vector $\mathbf{f}$ and time function $u(t)$

$$\mathbf{F}(t) = \mathbf{f}u(t) \tag{1}$$

If the modal vectors are mass-ortho-normalized such that

$$\mathbf{V}^T\mathbf{K}\mathbf{V} = \mathbf{\Omega} \tag{2a}$$

$$\mathbf{V}^T\mathbf{M}\mathbf{V} = \mathbf{I} \tag{2b}$$

the flexibility matrix then can be represented using the modal parameters (Doebling 1995)

$$\mathbf{F} = \mathbf{K}^{-1} = \mathbf{V}\mathbf{\Omega}^{-1}\mathbf{V}^T \tag{3}$$

where $\mathbf{\Omega}$ = spectral matrix with the diagonal entries being the eigenvalues of the system; and $\mathbf{V}$ = modal matrix for the corresponding eigenvectors. The flexibility matrix can be divided into two parts: the modal flexibility $\mathbf{F}_m$, which is formed from the measured frequencies and modal vectors, and the residual flexibility $\mathbf{F}_r$ formed from the unmeasured residual modes (Doebling 1995)

$$\mathbf{F} = \mathbf{F}_m + \mathbf{F}_r = \mathbf{V}_m\mathbf{\Omega}_m^{-1}\mathbf{V}_m^T + \mathbf{V}_r\mathbf{\Omega}_r^{-1}\mathbf{V}_r^T \tag{4}$$

where the subscripts m and r denote the measured and residual quantities, respectively. Note that the contributions of the lower modes, which are normally estimated in experimental modal analyses, are more significant than those of the higher modes because the contribution of each mode to the flexibility matrix is inversely proportional to the magnitude of the corresponding natural frequency. Therefore, the complete flexibility matrix is approximated by the modal flexibility matrix; i.e., $\mathbf{F} = \mathbf{V}_m\mathbf{\Omega}_m^{-1}\mathbf{V}_m^T$. It has been reported that the contribution of the residual flexibility is generally about 3–10% of the modal flexibility matrix (Doebling 1995).

Using the modal flexibility matrix $\mathbf{F}_m$ and the analytical mass matrix $\mathbf{M}$, the first Ritz vector can be computed

$$\bar{\mathbf{r}}_1 = \mathbf{F}_m\mathbf{f} \tag{5}$$

where $\mathbf{f}$ = spatial load distribution vector defined in (1). The first Ritz vector is then mass normalized

$$\mathbf{r}_1 = \frac{\tilde{\mathbf{r}}_1}{[\tilde{\mathbf{r}}_1^T\mathbf{M}\tilde{\mathbf{r}}_1]^{1/2}} \tag{6}$$

The subsequent Ritz vectors are generated using the following recursive relationship:

$$\bar{\mathbf{r}}_s = \mathbf{F}_m \mathbf{M} \mathbf{r}_{s-1} \tag{7}$$

The linear independence of Ritz vectors is achieved using the Gram-Schmidt orthogonalization

$$\tilde{\mathbf{r}}_s = \bar{\mathbf{r}}_s - \sum_{t=1}^{s-1} (\mathbf{r}_t^T \mathbf{M} \bar{\mathbf{r}}_s) \mathbf{r}_t \tag{8}$$

Finally, the current Ritz vector is mass normalized

$$\mathbf{r}_s = \frac{\tilde{\mathbf{r}}_s}{[\tilde{\mathbf{r}}_s^T \mathbf{M} \tilde{\mathbf{r}}_s]^{1/2}} \tag{9}$$

It is worth briefly comparing the flexibility-based extraction procedure with the state-space–based procedure proposed by Cao and Zimmerman (1997b). The state-space approach requires the information regarding the actual load pattern used in the vibration test. Therefore, the state-space–based method only identifies the Ritz vectors corresponding to the specific excitation pattern used in the actual modal testing. Because the spatial load distribution vector **f** in (5) can be assigned arbitrarily, the flexibility method described here is able to generate different sets of Ritz vectors. Note that both methods require an appropriate approximation for the mass matrix. However, because stiffness changes are the main concern for the damage detection problem, the exact estimation of the mass matrix is not necessarily an important issue.

TABLE 1. Comparison of Analytical and Experimental Natural Frequencies

Mode	Frequency (Hz)		Relative error[a] (%)
	Analytical ω	Experimental $\hat{\omega}$	
1st bending	5.4488	5.5635	2.06
1st torsion	10.1494	10.0406	1.08
2nd bending	19.1841	18.6410	2.91
2nd torsion	30.6216	29.4388	4.02
3rd bending	41.6086	42.5910	2.31
3rd torsion	54.9704	57.1864	3.88

[a]Error = $|\omega - \hat{\omega}|/\hat{\omega}$.

ANALYTICAL MODELING OF TEST STRUCTURE

A finite-element (FE) model for the grid-type bridge structure is constructed using 20 3D beam elements. As shown in Fig. 2, a girder segment between two nodes or a cross beam is modeled as a single element. Fourteen beam elements in the two girders are numbered consecutively from node 1 to node 16. Then, the six cross beams are numbered from left to right. An elastic modulus of 2.0×10^5 MPa, mass density of 7,850 kg/m^3, and Poisson's ratio of 0.2 are specified for the model. Because the accelerometers measure only the vertical movement of the structure, the lateral degrees of freedom (DOF) are not included in the analytical model. Therefore, such node of an element has two translational DOF and three rotational DOF. The model has a total of 64 DOF, including four rotational DOF at the boundary. Both ends of the beam are modeled as simple pinned connections. A pinned connection is modeled by a ball bearing with a 35-mm diameter in the experimental setup. Based on a preliminary vibration test, the boundary conditions appear to be less accurately modeled. The boundary conditions are then modified by introducing rotational springs at the rotational DOF. Furthermore, additional springs are added to the rotational DOF at both ends of the cross beams to simulate the bolted connection between the girders and the cross beams. After these modifications, the

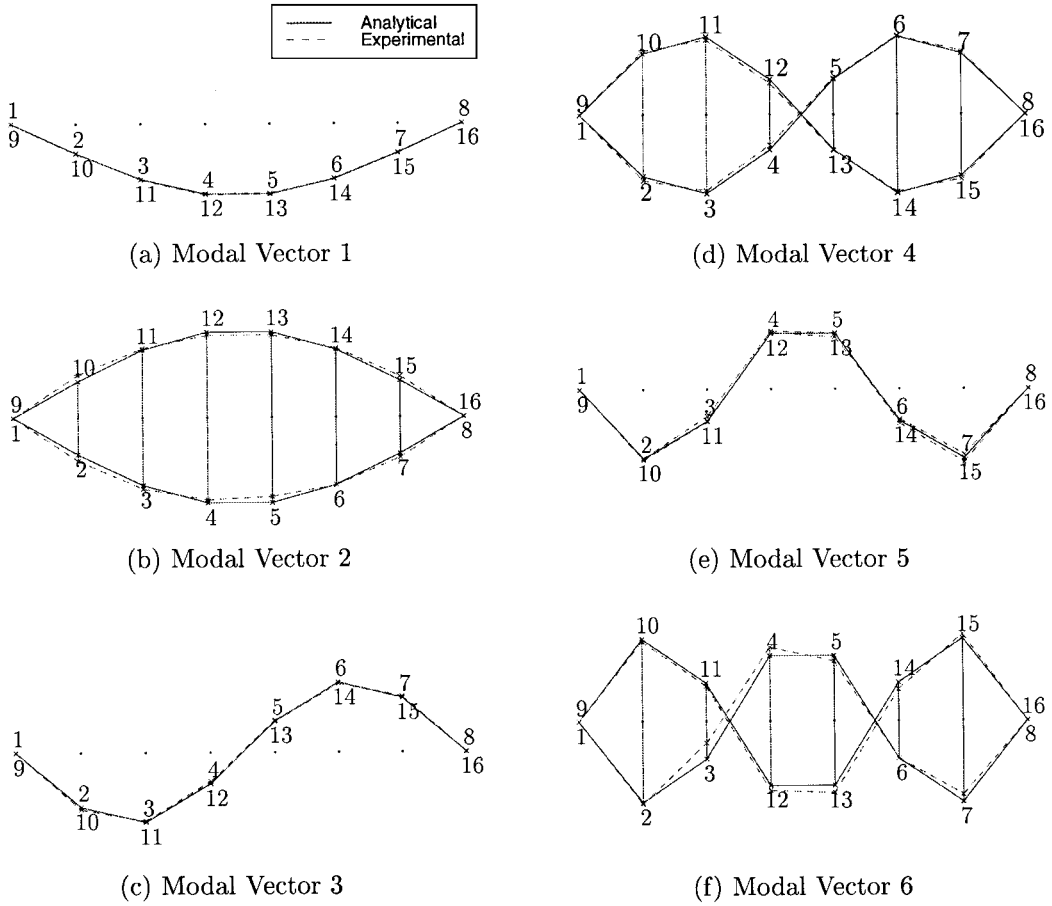

FIG. 3. Analytical and Experimental Modal Vectors

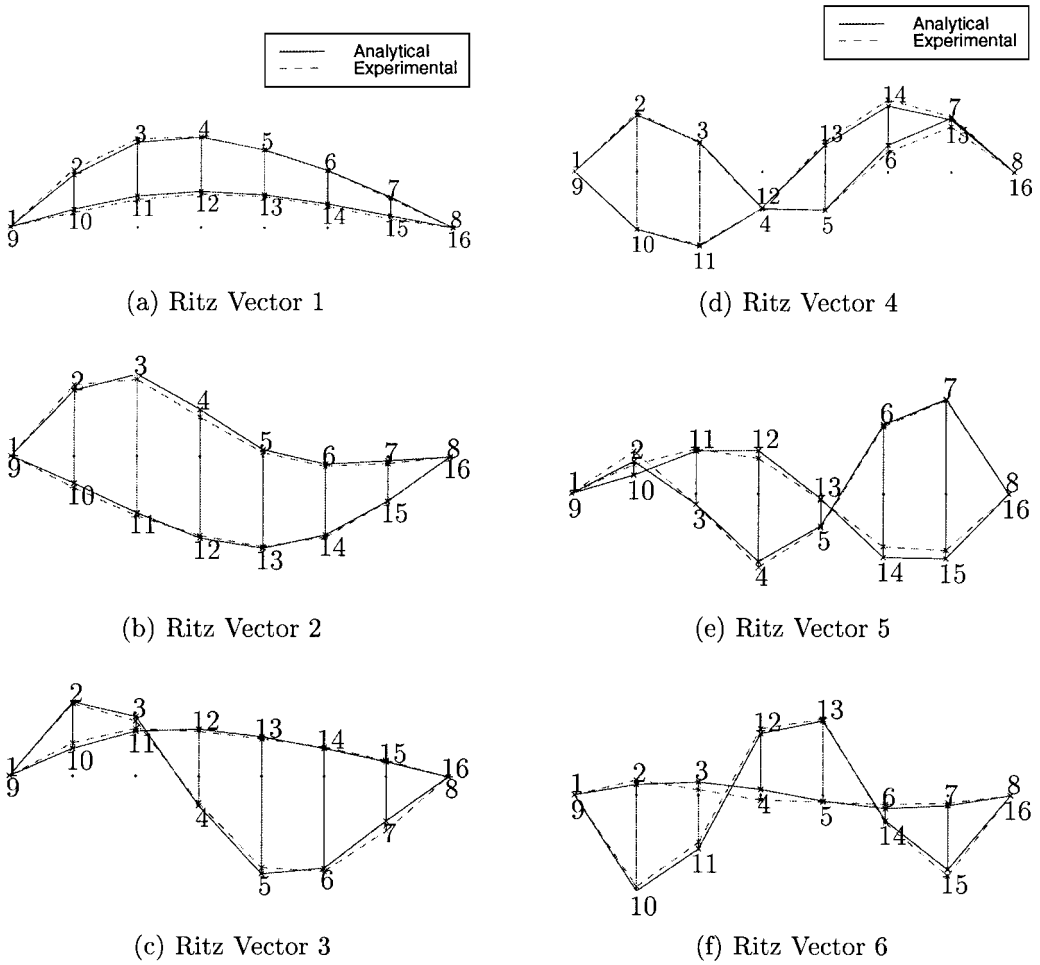

FIG. 4. Comparison of Analytical and Experimental Ritz Vectors

relative errors of the first six natural frequencies between the analytical model and the test structure fall within 4%.

Table 1 compares the values of the analytical and experimental natural frequencies. Here, the experimental frequency $\hat{\omega}$ is a mean value of the three frequencies estimated with an impact load applied at nodes 3–5, one at a time. Fig. 3 displays the analytical and experimental modal vectors of the first six modes. For all figures of modal and Ritz vectors, the structure is viewed from the side.

Fig. 4 also shows the first six analytical and experimental Ritz vectors with an impulse excitation at node 3. The experimental Ritz vectors are computed following the extraction procedure described earlier, and the analytical Ritz vectors are computed using the procedure described in Sohn and Law (2001). Note that the first Ritz vector is equivalent to a deflection pattern observed when a unit load is applied to node 3.

As for the scaling of the Ritz or modal vectors, a mass normalization is conducted. However, because the DOF of the analytical model do not coincide with the DOF of the experimental Ritz or modal vectors, a reduced analytical mass matrix is first constructed using the Guyan (static) condensation procedure. Then, both the analytical and the experimental vectors are normalized with respect to the reduced mass matrix. Errors arising from the model reduction are found to be minimum because the inertial forces associated with the omitted rotational and axial DOF (slave DOF) are negligible in this example.

BAYESIAN FRAMEWORK FOR DAMAGE DETECTION

A Bayesian framework is applied to diagnose the damages imposed on the test structure (Sohn and Law 1997). For an analytical model with N_{sub} substructures, the system stiffness matrix $\mathbf{K}$ can be expressed as an assembly of substructure stiffness matrices $\mathbf{K}_{si}$

$$\mathbf{K}(\Theta) = \sum_{i=1}^{N_{\text{sub}}} \theta_i \mathbf{K}_{si} \tag{10}$$

where $\Theta = \{\theta_i;\ i = 1, \ldots, N_{\text{sub}}\}$ and θ_i $(0 \leq \theta_i \leq 1)$ = nondimensional parameter, which represents the contribution of the ith substructure stiffness to the system stiffness matrix. A substructure is defined as damaged when the θ value is less than a specified threshold.

When vibration tests are repeated N_s times, the total collection of N_s data sets is denoted

$$\hat{\Psi}_{N_s} = \{\hat{\psi}(n):\ n = 1, \ldots, N_s\} \tag{11}$$

Each data set $\hat{\psi}(n)$ is composed of the Ritz (or modal) vectors estimated from the nth vibration test

$$\hat{\psi}(n) = [\hat{\mathbf{r}}_1^{nT}, \ldots, \hat{\mathbf{r}}_{N_r}^{nT}]^T \in \mathbf{R}^{N_t} \tag{12}$$

where $\hat{\mathbf{r}}_i^n$ denotes the ith estimated Ritz vector (or modal) in the nth data set $\hat{\psi}(n)$. The vector $\hat{\mathbf{r}}_i^n$ $(\hat{\mathbf{r}}_i^n \in \mathbf{R}^{N_d})$ has components corresponding to the instrumented DOF. The variables N_t, N_d, and N_r represent the total number of components in a data set $\hat{\psi}(n)$, number of measured DOF, and number of estimated vectors, respectively.

Let H_j denote a hypothesis for a damage event that can contain any number of substructures as damaged. The initial degree of belief about the hypothesis H_j is represented by a prior probability $P(H_j)$. Using Bayes' theorem, the posterior

probability $P(H_j|\hat{\Psi}_{N_s})$, after observing the estimated data sets $\hat{\Psi}_{N_s}$, is given

$$P(H_j|\hat{\Psi}_{N_s}) = \frac{P(\hat{\Psi}_{N_s}|H_j)}{P(\hat{\Psi}_{N_s})} P(H_j) \tag{13}$$

The most likely damaged substructures are the ones included in the hypothesis $H_{\max}$, which has the largest posterior probability; i.e.

$$P(H_{\max}|\hat{\Psi}_{N_s}) = \max_{\forall H_j} P(H_j|\hat{\Psi}_{N_s}) \tag{14}$$

Because the objective is to determine the most probable damage hypothesis (event), only the relative posterior probabilities of alternative hypotheses are of interest. One attempts to avoid the explicit expression of a posterior probability $P(H_j|\hat{\Psi}_{N_s})$ because the precise calculation of $P(\hat{\Psi}_{N_s}|H_j)$ is a difficult task. To overcome this difficulty, one focuses on the relative comparisons of posterior probabilities.

Note that the search of the most likely damage hypothesis in (14) theoretically require the examination of all possible damage scenarios. A branch-and-bound search scheme has been proposed, using bounding heuristics to expedite the search without exhaustively examining all the possible damage hypotheses (Sohn and Law 1997). If the damages are localized in a few substructures, the number of damage hypotheses that need to be examined by the branch-and-bound search is relatively small and the search becomes computationally feasible.

DAMAGE DETECTION USING EXPERIMENTAL DATA

Continuous deterioration of stiffness is simulated at three different regions of the grid structure and the vibration tests are conducted at six different damage stages, as shown in Table 2. The three damage locations (elements 2, 6, and 11) are indicated as shown in Fig. 2. First, a single damage is introduced at damage location 1 (for cases 1 and 2) and the second damage is formed between nodes 12 and 13 (for cases 3–5). Finally, damage case 6 is simulated by adding damage location 3. For each damage location, a crack is introduced by a saw cutting at a distance of 30 cm to the left of a node, as shown in Fig. 5. For example, the damage location 1 in Fig. 2 is formed at 30 cm left to node 3. The severity of saw cutting in terms of depth (cm) and the percentage ratio of the cut depth to the height of the beam are tabulated as shown in Table 2. Table 3 summarizes the frequencies estimated at each damage stage.

TABLE 2. Description for Six Damage Cases of Grid-Type Bridge Structure

Case	Location 1[a]	Location 2[a]	Location 3[a]
1	2.0 cm (40%)	—	—
2	3.0 cm (60%)	—	—
3	3.0 cm (60%)	1.5 cm (30%)	—
4	3.0 cm (60%)	2.6 cm (52%)	—
5	3.0 cm (60%)	3.2 cm (64%)	—
6	3.0 cm (60%)	3.2 cm (64%)	2.5 cm (50%)

[a]Damage locations 1–3 are shown in Fig. 2. First number is depth of cut and second number is ratio of cut depth to height of beam (5 cm).

As for comparison, the damage diagnosis results using the six estimated modal vectors are presented first. For each damage stage, three sets of modal data, which are obtained from the impulse excitations at nodes 3–5, are employed using the Bayesian approach described earlier. The diagnosis results are summarized in Table 4. In the table, the column under $\hat{L}_{\text{dam}}$ shows the most likely damaged locations identified by the branch-and-bound search scheme. Because a preliminary sensitivity analysis shows that the measured modal parameters are insensitive to the stiffness changes of the cross-beam elements, the branch-and-bound search is conducted including only the 14 elements within the two girders. The first number in the column ''Rank'' denotes the highest rank among the damage events that include all the actual damage locations, which may also include other ''erroneous'' damage locations, and the second number presents the rank of the actual damage event. The results show that at the final damage stage the diagnosis employing the modal parameters converges to the actual damage locations.

The same six damage cases are rediagnosed using the Ritz vectors generated from different load patterns using the measured modal flexibility matrix. A point load is assumed to be applied to the vertical direction of each node and the first six Ritz vectors are generated from each load pattern. This process is repeated for all 12 vertical DOF and a total of 72 (6 Ritz vectors/load $\times$ 12 load patterns) Ritz vectors are generated. Note that, following the proposed extraction procedure, Ritz vectors corresponding to any load pattern can be theoretically extracted with the same amount of test data used to estimate the modal parameters.

The diagnosis results using the Ritz vectors are also sum-

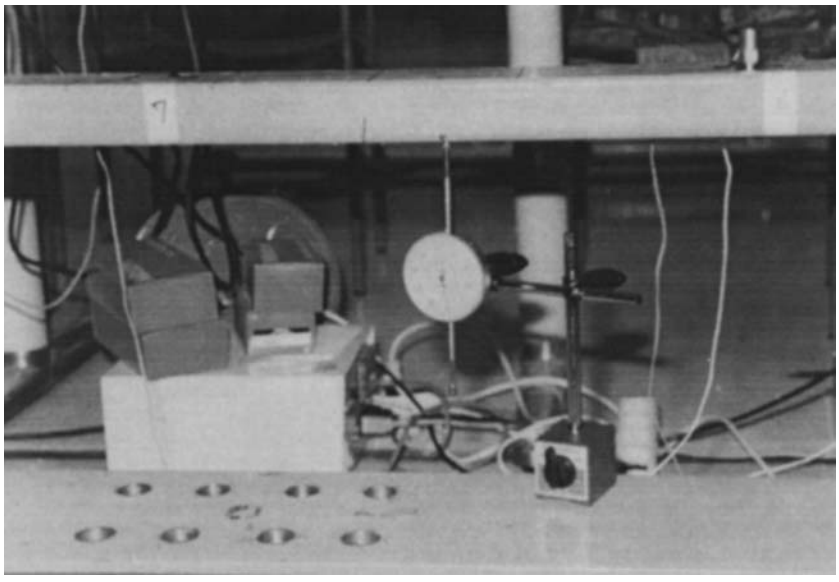

FIG. 5. Actual Damage Introduced to Grid-Type Bridge Structure

marized in Table 4. For cases 1 and 2, the actual damage event is ranked as the 2nd and 12th most likely damage event, respectively. In the first two cases, damage location 1 is included in the most likely damage event estimated by the branch-and-bound search. That is, although the branch-and-bound search fails to pinpoint the actual damage location, the search finds the actual damage location as one of the most likely damage locations. For case 3, the actual damage event is ranked as the ninth most likely event. For case 4, the actual damage case is ranked as the third most likely event. For cases 5 and 6, the branch-and-bound search finds the actual damage events as the most probable ones.

TABLE 3. Natural Frequencies (Hz) Estimated at Different Damage Levels

Damage case	Natural Frequency (Hz)					
	1st	2nd	3rd	4th	5th	6th
0	5.5635	10.0406	18.6410	29.4388	42.5910	57.1864
1	5.5325	9.8055	18.0557	29.0354	42.0302	56.6170
2	5.4834	9.6725	17.2749	28.5032	41.1840	56.1848
3	5.3699	9.5971	17.2364	27.6911	40.6107	55.3881
4	5.2398	9.5249	17.2193	27.3410	39.7738	52.3992
5	5.0254	9.3938	17.1694	27.1571	38.5939	51.6392
6	4.9622	9.0075	16.1835	26.6957	37.2933	49.9543

TABLE 4. Damage Diagnosis Results for Grid-Type Structure Using Ritz and Modal Vectors

Case	Damage location	Ritz Vectors		Modal Vectors	
		$\hat{L}_{\text{dam}}$[a]	Rank[b]	$\hat{L}_{\text{dam}}$[a]	Rank[b]
1	{2}	{2, 3}	1 (2)	{2, 8, 9}	1 (29)
2	{2}	{2, 3}	1 (12)	{2, 8, 12}	1 (46)
3	{2, 11}	{2, 3}	3 (9)	{2, 3, 8}	13 (41)
4	{2, 11}	{2}	3 (3)	{2, 8, 12}	4 (12)
5	{2, 11}	{2, 11}	1 (1)	{2, 11, 12}	1 (9)
6	{2, 6, 11}	{2, 6, 11}	1 (1)	{2, 6, 11}	1 (1)

[a]$\hat{L}_{\text{dam}}$ is set of most probable damage locations identified by branch-and-bound search.

[b]First number is highest rank of damage event, which includes all actual damage locations, and second number in parentheses is rank of actual damage event.

TABLE 5. Diagnosis Result for Damage Case 3 of Girder Structure

Rank	$\hat{L}_{\text{dam}}$
1	{2, 3}
2	{2, 3, 4}
3	{2, 3, 11}
4	{2, 3, 12}
5	{2}
6	{2, 4}
7	{1, 2, 3}
8	{2, 12}
9	{2, 11}

Table 5 shows the first nine most probable damage events identified by the branch-and-bound search for damage case 3. The first two most probable events only include damage location 1 (element 2) and miss damage location 2 (element 11). However, the third most probable event includes the two damage locations and one extra element 3. That is, although the proposed approach ranks the actual damage event as the ninth most probable event, the third most likely event conservatively includes all the actual damage locations.

The results shown in Table 4 indicate that the Ritz vectors provide better diagnosis results for the six damage cases investigated than the modal vectors. In Fig. 6, the sensitivity comparison using the experimental Ritz and modal vectors at different damage stages is conducted. This figure shows the normalized Euclidean norm difference between the ''healthy'' vectors ($\mathbf{r}^h$ or $\mathbf{v}^h$) and the vector at each damage stage ($\mathbf{r}^d$ or $\mathbf{v}^d$). The Ritz vectors employed for the comparison are those extracted from a point load applied at node 3. It can be seen that a careful selection of load patterns can make damages more observable. The better sensitivity of Ritz vectors to damage locations and the increased amount of information employing multiple load patterns seem to provide better damage diagnosis than using a single invariant set of modal vectors.

Finally, using the test data obtained from case 5, Fig. 7 illustrates the branch-and-bound search scheme proposed in Sohn and Law (1997). The branch-and-bound search finds the actual damage event as the most likely one after examining 63 different damage scenarios out of 16,384 ($=2^{14}$) possible combinations of damage scenarios.

COMPARISON WITH OTHER DAMAGE DETECTION METHODS

The Minimum Rank Perturbation Theory (MRPT) (Kaouk and Zimmerman 1994) and the Sensitivity-Based Element-by-Element (SB-EBE) method (Farhat and Hemez 1993) are employed for comparison in this study. A brief description of these methods is summarized in the following subsections.

MRPT Method

The MRPT method proposed by Kaouk and Zimmerman (1994) consists of two basic steps. First, dynamic residual forces (also known as damage vectors or residual force vectors) are employed to locate the damaged regions, which are mathematically expressed in terms of the DOF in the analytical model. Second, the lowest rank perturbation is introduced to the analytical stiffness matrix such that the residual forces are

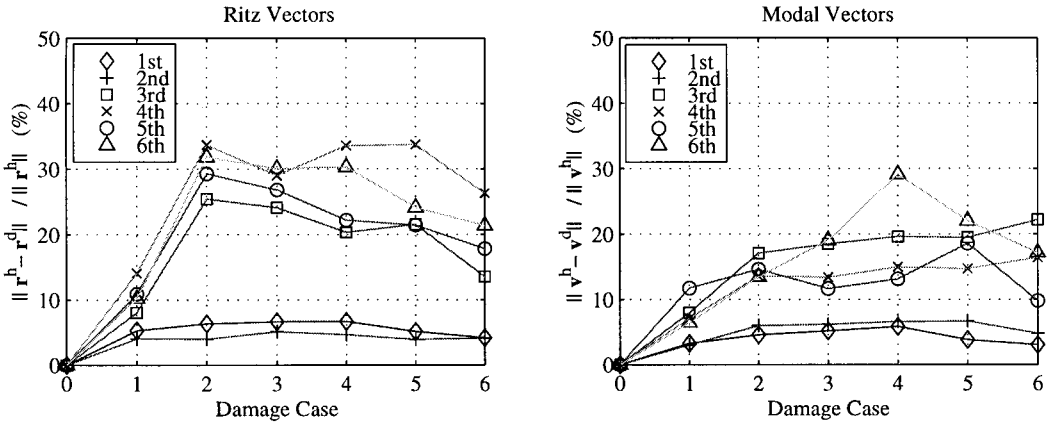

FIG. 6. Sensitivity Comparison of Ritz and Modal Vectors at Different Damage Stages

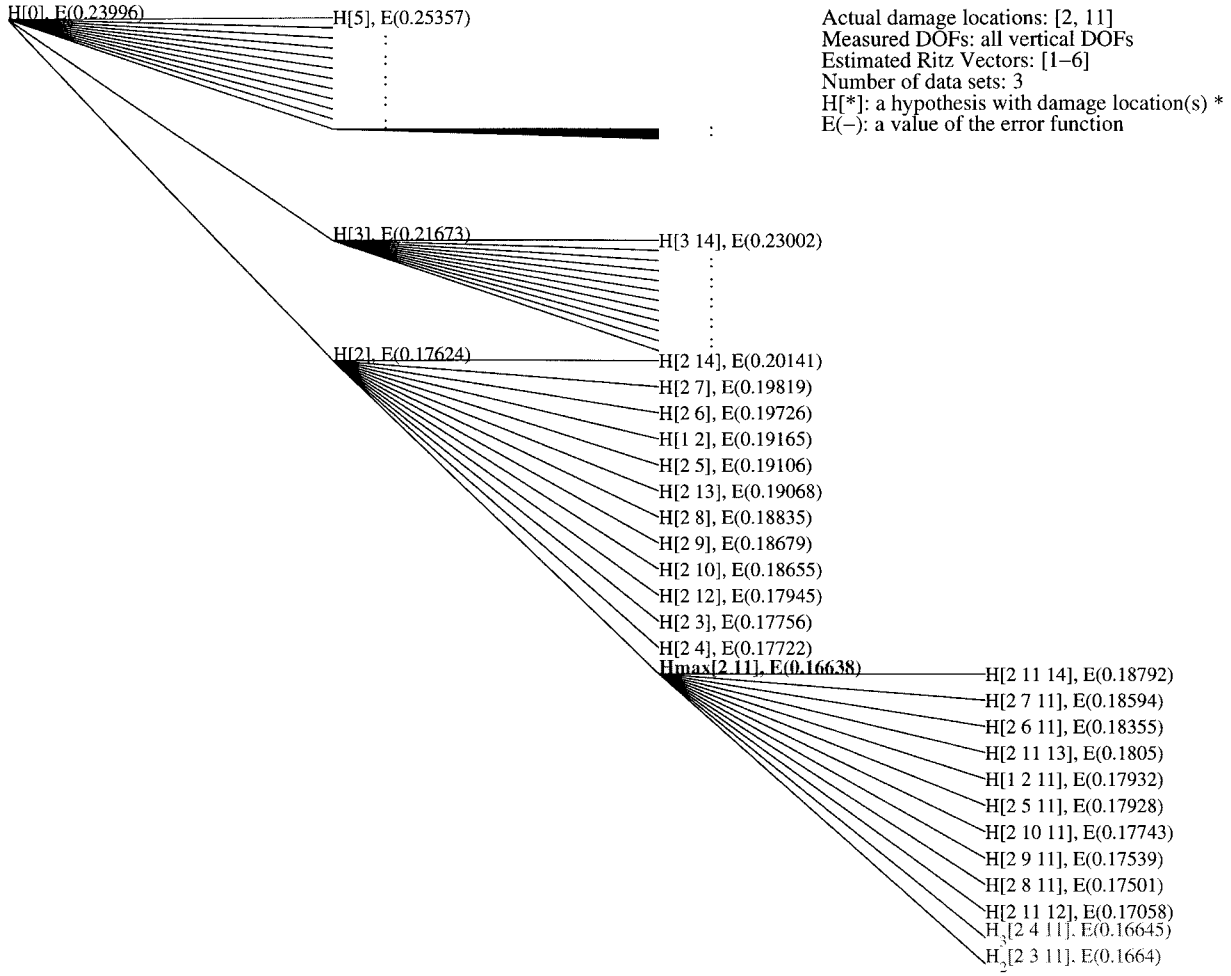

FIG. 7. Branch-and-Bound Search of Grid-Type Bridge Model

minimized. This method is computationally efficient and does not require any iteration. However, the measurement points of the experimental modal vectors should coincide with those of the analytical model and the dimension of the modal vectors should be the same as the dimension of the analytical model. To satisfy these conditions, the Guyan condensation is applied to the analytical model. The MRPT method can be extended for the case where multiple data sets are available from several static and vibration tests (Zimmerman and Simmermacher 1995).

Using all three modal data sets obtained at each damage stage of the grid structure, Fig. 8 summarizes the diagnosis results obtained by the extended MRPT method (Zimmerman and Simmermacher 1995). In this figure, the abscissa shows the node numbers of the bridge model as defined in Fig. 2, and the ordinate displays the changes of the diagonal components of the stiffness matrix at each damage stage. The expressions $\mathbf{K}_{ii}^{h}$ and $\mathbf{K}_{ii}^{d}$ denote the stiffness coefficient for node i before and after damage occurrence, respectively. Note that each node has one vertical degree of freedom after the condensation and the stiffness change is normalized such that the maximum change is 1. The end nodes for each damaged member are distinguished by a darker color in the figure. It can be seen from the results that the damages are not consistently recognized.

SB-EBE Method

The SB-EBE method proposed by Farhat and Hemez (1993) searches for the locations of potential errors between the FE model and the measured modal data, and then updates the analytical model at the element level by adjusting the elements' material properties. This method minimizes the squared norms of the modal dynamic residuals by means of a two-step iteration: At each iteration, the estimated modal vectors are first expanded and the parameters of the elements are corrected using the expanded modal vectors and natural frequencies. The SB-EBE method seems to be appropriate here because the mode shape expansion scheme is built within the updating process and damage can be identified at each structural element level. Because this method is designed to employ a single modal parameter set for updating and three sets of modal parameters are experimentally obtained for each damage case, the diagnosis is repeated three times for each damage case. Fig. 9 shows the best diagnosis result using three different modal data sets. In this figure, the abscissa represents the element number and the ordinate denotes the percentage change of the corresponding substructure stiffness. It can be observed that the method is partially successful in identifying significant changes in some of the damage locations, but a number of the actual damage locations show very little stiffness changes.

SUMMARY AND DISCUSSIONS

This paper describes the potential application of load-dependent Ritz vectors and their incorporation into the previously proposed Bayesian framework for damage diagnosis. A procedure that extracts the Ritz vectors based on a flexibility matrix estimated from experimentally obtained modal parameters has also been presented. The main advantage of the flexibility-based extraction procedure is that the method can generate Ritz vectors from arbitrary load patterns. Damage

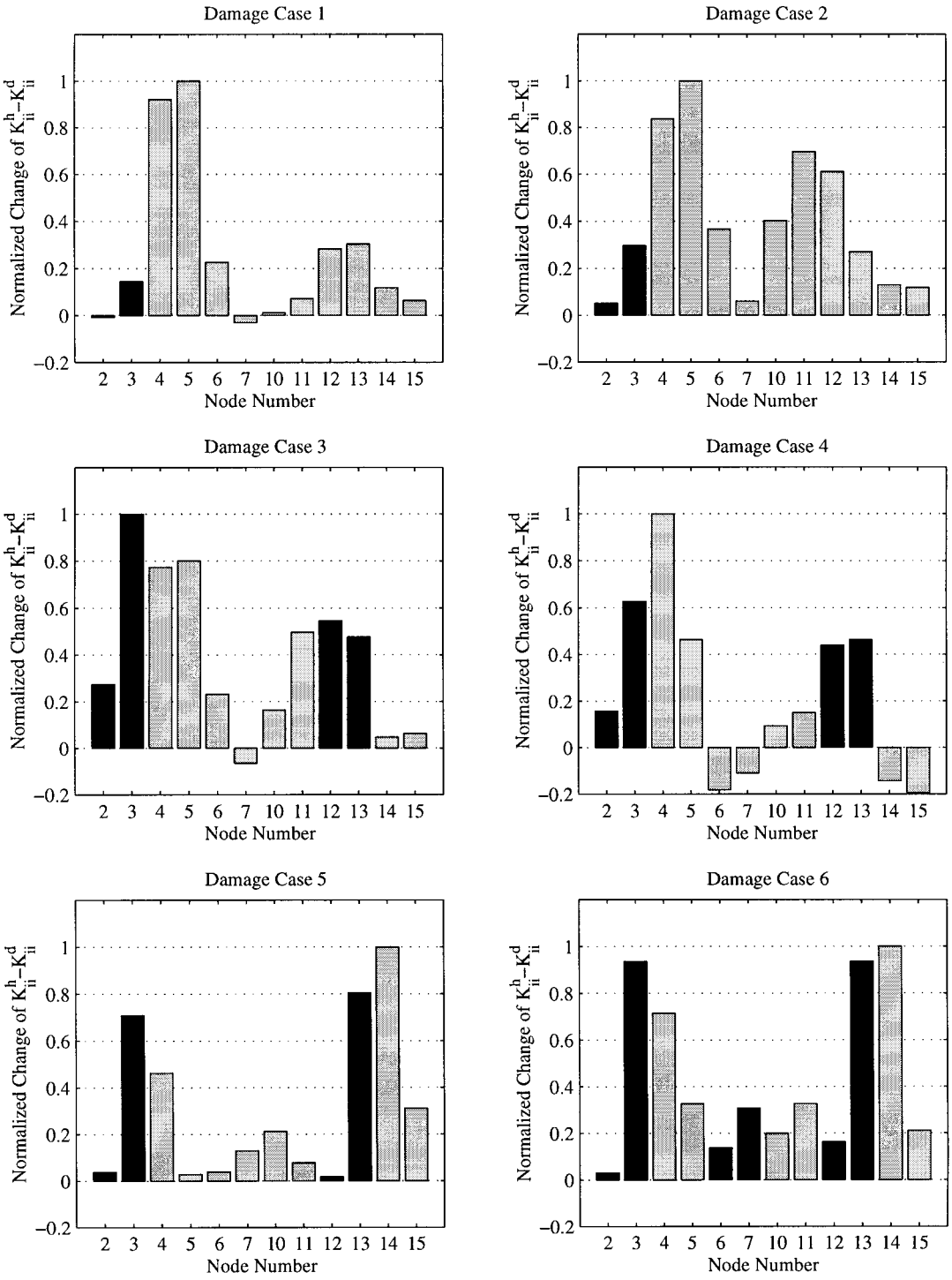

FIG. 8. Damage Diagnosis of Bridge Model Using MRPT Method

diagnoses of the grid-type bridge model indicate that the employment of Ritz vectors provides better indication of the actual damage locations than using the modal vectors. The superior performance of Ritz vectors over modal vectors is attributed to (1) the better sensitivity of Ritz vectors over modal vectors; and (2) the increased amount of information obtained by employing multiple load patterns.

As for comparison, the results from the application of the MRPT and SB-EBE methods to the test data of the grid structure are also presented. The MRPT method requires a decision on the rank of the stiffness perturbation that is added to the original stiffness matrix, and the performance of the MRPT method greatly depends on the rank selection. In this study, the rank is decided based on the knowledge of the actual damage locations. However, for real applications, the rank will be selected without the knowledge of damage locations. The SB-EBE method provides a better diagnosis result than the MRPT method and identifies damage amount as well as damage locations. However, the SB-EBE method can only employ one modal parameter set at a time and the diagnosis result varies drastically depending on which modal parameter set is used. Therefore, the SB-EBE method may not be suitable for the continuous monitoring that is the aim in this study.

The MRPT and SB-EBE methods have originally been developed in the field of aerospace industry for the monitoring of space-station–like structures such as truss structures. These algorithms, including the one proposed here, require complementary FE models for damage diagnosis. A further study is

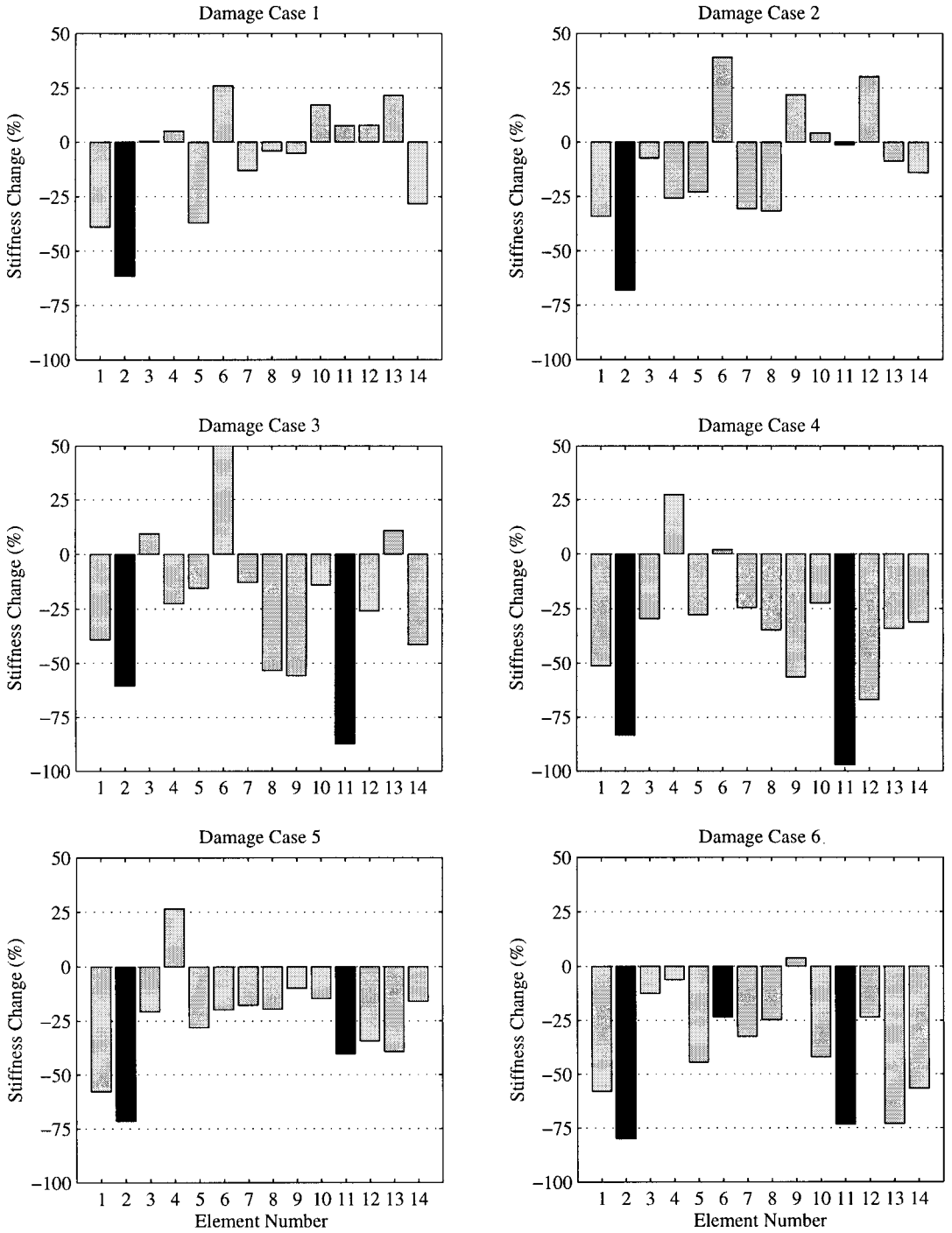

FIG. 9. Damage Diagnosis of Bridge Model Using SB-EBE Method

necessary to fully address the issues that arise in the monitoring of civil structures. For example, civil structures involve a significant amount of uncertainties caused by environmental effects such as temperature, loading, and humidity. These changes are shown possibly to be several times the modal property changes expected from structural damage. In addition, civil structures typically display more complicated geometry; consist of many different materials such as steel, concrete, cable and asphalt; and involve more redundancy in the design than space structures. These issues make the accurate modeling of civil structures very difficult.

ACKNOWLEDGMENTS

This research is partially sponsored by the National Science Foundation, Washington, D.C., under Grant No. CMS-95261-2. The writers wish to express their sincere thanks to Hyundai Engineering & Construction Co. Ltd., Kyunggi-Do, South Korea, for inviting the first writer to participate in the test of the grid-type bridge model and to Dr. Chuck R. Farrar and Dr. Scott W. Doebling of the Los Alamos National Laboratory for providing the DIAMOND software. The first writer also would like to thank Dr. Jeong Hwan Jang of Seoul National University for his contributions to the experimental study.

REFERENCES

Cao, T. T., and Zimmerman, D. C. (1997a). ''Application of load-dependent Ritz vectors in structural damage detection.'' *Proc., 15th Int. Modal Anal. Conf.*, Society of Experimental Mechanics, Inc., Orlando, Fla., 1319–1324.

Cao, T. T., and Zimmerman, D. C. (1997b). ''A procedure to extract Ritz vectors from dynamic testing data.'' *Proc., 15th Int. Modal Anal. Conf.*, Society of Experimental Mechanics, Inc., Orlando, Fla., 1036–1042.

Carey, C. M. M., Golub, G. H., and Law, K. H. (1994). ''A Lanczos-

based method for structural dynamic reanalysis problems.'' *Int. J. Numer. Methods in Engrg.*, 37, 2857–2883.
Doebling, S. W. (1995). ''Measurement of structural flexibility matrices for experiments with incomplete reciprocity.'' PhD thesis, Aerospace Engrg. Sci., University of Colorado, Boulder, Colo.
Doebling, S. W., Farrar, C. R., Prime, M. B., and Shevitz, D. W. (1996). ''Damage identification and health monitoring of structural and mechanical systems from changes in their vibration characteristics: A literature review.'' *Tech. Rep. LA-13070-MS*, Los Alamos National Laboratory, Los Alamos, N.M.
Farhat, C., and Hemez, F. M. (1993). ''Updating finite element dynamic model using an element-by-element sensitivity methodology.'' *Am. Inst. of Aeronautics and Astronautics*, 31, 1702–1711.
Golub, G. H., and Loan, C. F. V. (1996). *Matrix computations*, Johns Hopkins University Press, Baltimore.
Kaouk, M., and Zimmerman, D. C. (1994). ''Structural damage assessment using a generalized minimum rank perturbation theory.'' *Am. Inst. of Aeronautics and Astronautics*, 32, 836–842.
Leger, P., Wilson, E., and Clough, R. (1986). ''The use of load-dependent Ritz vectors for dynamic and earthquake analyses.'' *Tech. Rep. UCB/EERC-86/04*, Earthquake Engrg. Res. Ctr., University of California Berkeley, Berkeley, Calif.
Nour-Omid, B., and Clough, R. W. (1984). ''Dynamics analysis of structures using Lanczos coordinates.'' *Earthquake Engrg. and Struct. Dyn.*, 12, 565–577.
Pandey, A. K., Biswas, M., and Samman, M. M. (1991). ''Damage detection from changes on curvature mode shapes.'' *J. Sound and Vibration*, 145, 321–332.
Raghavendrachar, M., and Aktan, A. E. (1992). ''Flexibility by multireference impact testing for bridge diagnostics.'' *J. Struct. Engrg.*, ASCE, 118(8), 2186–2203.
Richardson, M. H., and Formenti, D. L. (1982). ''Parameter estimation form frequency response measurements using rational fraction polynomials.'' *Proc., 1st Int. Modal Anal. Conf.*, Society of Experimental Mechanics, Inc., Orlando, Fla., 167–181.
Sohn, H., and Law, K. H. (1997). ''Bayesian probabilistic approach for structure damage detection.'' *Earthquake Engrg. and Struct. Dyn.*, 26, 1259–1281.
Sohn, H., and Law, K. H. (2000). ''Application of load-dependent Ritz vectors to Bayesian probabilistic damage detection.'' *Probabilistic Engrg. Mech.*, 15(2), 139–153.
Sohn, H., and Law, K. H. (2001). ''Extraction of Ritz vectors from vibration test data.'' *Mech. Sys. and Signal Processing*, 15(1), 213–226.
Topole, K. G., and Stubbs, N. (1995). ''Nondestructive damage evaluation of a structure from limited modal parameters.'' *Earthquake Engrg. and Struct. Dyn.*, 24, 1427–1436.
Yao, G. C., Chang, K. C., and Lee, G. C. (1992). ''Damage diagnosis of steel frames using vibrational signature analysis.'' *J. Engrg. Mech.*, ASCE, 118(8), 1949–1961.
Zimmerman, D. C., and Simmermacher, T. (1995). ''Model correlation using multiple static load and vibration tests.'' *Am. Inst. of Aeronautics and Astronautics*, 33, 2182–2188.